

1 **Contrasting inflammatory signatures in peripheral blood and bronchoalveolar cells**  
2 **reveal compartment-specific effects of HIV infection.**

3

4 Daniel M. Muema<sup>1,2,3\*</sup>, Maphe Mthembu<sup>1\*</sup>, Abigail Schiff<sup>4,5</sup>, Urisha Singh<sup>1</sup>, Björn  
5 Corleis<sup>4,6</sup>, Thierry Bassett<sup>1</sup>, Siphso S. Rasehlo<sup>1</sup>, Kennedy Nyamande<sup>7</sup>, Dilshaad Fakey Khan<sup>7</sup>,  
6 Priya Maharaj<sup>7</sup>, Mohammed Mitha<sup>7</sup>, Moosa Suleman<sup>7</sup>, Zoey Mhlane<sup>1</sup>, Taryn Naidoo<sup>1</sup>,  
7 Dirhona Ramjit<sup>1</sup>, Farina Karim<sup>1</sup>, Douglas S. Kwon<sup>2,4</sup>, Thumbi Ndung'u<sup>1,2,4,8,9</sup> and Emily B.  
8 Wong<sup>1,5,8,10</sup>

9

10 <sup>1</sup>African Health Research Institute, Durban, South Africa,

11 <sup>2</sup>HIV Pathogenesis Programme, The Doris Duke Medical Research Institute, University of  
12 KwaZulu-Natal, Durban, South Africa,

13 <sup>3</sup>KEMRI-Wellcome Trust Research Programme, Kenya,

14 <sup>4</sup>Ragon Institute of MGH, MIT and Harvard, Cambridge, USA,

15 <sup>5</sup>Harvard Medical School, Boston, MA, USA,

16 <sup>6</sup>Institute of Immunology, Friedrich-Loeffler-Institute, Federal Research Institute of Animal  
17 Health, Greifswald, Isle of Riems, Germany,

18 <sup>7</sup>Department of Pulmonology, Inkosi Albert Luthuli Central Hospital, Nelson R Mandela  
19 School of Medicine, College of Health Sciences, University of KwaZulu-Natal, Durban,  
20 South Africa,

21 <sup>8</sup>Division of Infection and Immunity, University College London, London, UK,

22 <sup>9</sup>Max Planck Institute for Infection Biology, Berlin, Germany,

23 <sup>10</sup>Division of Infectious Diseases, Massachusetts General Hospital, Boston, USA.

24 \* These authors contributed equally

25 Corresponding author:

26 Dr. Emily B Wong

27 Africa Health Research Institute

28 719 Umbilo Road, Durban 4001

29 South Africa

30 Email: [emily.wong@ahri.org](mailto:emily.wong@ahri.org)

31 Telephone: +27-31-2604899

32 Fax: +27-31-2604203

33

34 The authors declare no conflict of interest.

35

36 **Abstract (199 words)**

37 The mechanisms by which HIV increases susceptibility to tuberculosis and other respiratory  
38 infections are incompletely understood. We used transcriptomics of paired whole  
39 bronchoalveolar lavage (BAL) fluid and peripheral blood mononuclear cells to compare the  
40 effect of HIV at the lung mucosal surface and in the peripheral blood. The large majority of  
41 HIV-induced differentially expressed genes (DEGs) were specific to either the peripheral or  
42 lung mucosa compartments (1,307/1,404, 93%). Type I interferon signaling was the dominant  
43 signature of DEGs in HIV-positive blood with a less dominant and qualitatively distinct type  
44 I interferon gene set expression pattern in HIV-positive BAL. DEGs in the HIV-positive  
45 BAL were significantly enriched for infiltration with cytotoxic CD8<sup>+</sup> T cells. Higher  
46 expression of representative transcripts and proteins in BAL CD8<sup>+</sup> T cells during HIV  
47 infection, including *IFNG* (IFN- $\gamma$ ), *GZMB* (Granzyme B) and *PDCDI* (PD-1), was confirmed  
48 by cell-subset specific transcriptional analysis and flow cytometry. Thus, we report that a  
49 whole transcriptomic approach revealed qualitatively distinct effects of HIV in blood and  
50 bronchoalveolar compartments. Further work exploring the impact of distinct type I  
51 interferon programs and CD8<sup>+</sup> T cells infiltration of the lung mucosa during HIV infection  
52 may provide novel insights into HIV-induced susceptibility to respiratory pathogens.

53

54

55 **Introduction**

56 HIV is a major cause of morbidity and mortality in sub-Saharan Africa. South Africa bears  
57 the highest burden globally with approximately 7.7 million people living with HIV in 2018 <sup>1</sup>.  
58 Introduction of immediate antiretroviral therapy (ART) following diagnosis has greatly  
59 improved long-term outcomes and life expectancy in people living with HIV. However, 46%  
60 of people living with HIV in South Africa are still viremic either because they don't know  
61 their HIV status or due to treatment failure <sup>1</sup>.

62 HIV-infected viremic patients are more likely to develop active tuberculosis (TB) from either  
63 new exposure to *M. tuberculosis* (Mtb) or reactivation of a pre-existing latent Mtb infection  
64 when compared to HIV-uninfected and HIV-infected non-viremic individuals <sup>2,3</sup>. T helper 1  
65 (Th1) polarized CD4<sup>+</sup> T cells that produce interferon gamma and TNF-alpha are thought to  
66 play a significant role in controlling TB infection, and their depletion in HIV-infected  
67 individuals may contribute to the increased risk of TB disease <sup>4,5</sup>. However, the risk of  
68 developing active TB increases even before significant CD4<sup>+</sup> T cell depletion, doubling  
69 within the first year of HIV infection, suggesting that other HIV-induced modulations of the  
70 immune system could contribute to the increased risk of TB in people with HIV <sup>6</sup>. Indeed,  
71 HIV infection has been shown to decrease the polyfunctional cytokine production in Mtb-  
72 specific CD4<sup>+</sup> T cells independent of CD4<sup>+</sup> T cell depletion <sup>7,8</sup>. Additionally, HIV infection  
73 is associated with reduced phagocytic potential of alveolar macrophages, an effect that could  
74 reduce the initial innate immune barrier to TB infection <sup>9</sup>.

75 Strategies to enhance control of Mtb in HIV-infected and uninfected persons are hindered by  
76 our limited understanding of the natural immunological control of Mtb and the mechanisms  
77 underlying progression from latent Mtb infection to disease. Hypothesis-driven targeted  
78 studies may miss important pathways that could inform the understanding of TB  
79 immunopathogenesis. In contrast, high throughput approaches have the potential to offer

80 unbiased insights into the immune defects mediated by HIV, and thus advance the field of TB  
81 immunopathogenesis. One such approach is harnessing genome wide transcriptomic data to  
82 provide mechanistic insights into the immunologic pathways that are defective in patients  
83 who are likely to get infected with TB or progress to active disease, such as HIV-positive  
84 patients<sup>10-14</sup>. The use of whole blood or unsorted peripheral blood mononuclear cells  
85 (PBMCs) in transcriptomic studies has the advantage of giving an overall picture of the  
86 immune profiles that are associated with development of TB. For instance, transcriptomic  
87 analyses of whole peripheral blood in tuberculosis has pointed to the development of a type 1  
88 interferon signature<sup>10</sup>. Notably, even though it is established that HIV disrupts lung  
89 immunity and increases risk of TB disease, these whole genome studies have not investigated  
90 the effect of HIV in the lung, the site of Mtb exposure; most of the work has been on samples  
91 from peripheral blood because they are easily accessible.

92 In this study, we assessed the differences in immune profiles between blood and the  
93 bronchoalveolar compartments using whole compartment and sorted CD8<sup>+</sup> T cells by RNA-  
94 seq and flow cytometry. We also assessed the compartment-specific effects of HIV to  
95 comprehensively explore and describe the immunological defects that could explain the  
96 increased lung comorbidities, especially TB disease, in HIV-infected individuals. We report  
97 that while HIV induces primarily a type I interferon signature in blood, its primary signature  
98 in the bronchoalveolar compartment is an induction of a cytotoxic CD8<sup>+</sup> T cell infiltrate.

99

## 100 **Results**

### 101 Population characteristics

102 We used matched blood and bronchoalveolar fluid samples that were collected from 19 HIV-  
103 negative participants (15 from the research bronchoscopy cohort and 4 from the hospital-

104 based cohort) and 11 HIV-positive participants (8 from the research bronchoscopy cohort and  
105 3 from the hospital-based cohort) (Table 1). The median age of all participants was 34 years  
106 and 50% of the participants were female. There were no significant differences in age or sex  
107 distribution between the HIV-negative and HIV-positive groups. All HIV-infected  
108 participants were ART-naïve. The median viral load for the HIV-infected group was 54,942  
109 (Interquartile range [IQR]: 18,743-174,293). The median CD4+ T-cell counts for the HIV-  
110 uninfected and HIV-infected groups were 1,048 (IQR: 854-1,352) and 353 (IQR: 173-576),  
111 respectively ( $p < 0.0001$ ).

112

### 113 Distribution of major immune cell populations in bronchoalveolar compartment and blood

114 To determine the HIV-specific effects on the distribution of major populations of immune  
115 cells within each anatomical compartment, we used matched samples from the  
116 bronchoalveolar compartment and blood to conduct two-way comparisons i.e. between  
117 disease states within each compartment (comparisons 1 and 2, Figure 1A) and between  
118 compartments (comparisons 3 and 4). We carried out differential cell counts to enumerate  
119 differences in distribution of key immune cell populations between the two compartments  
120 (Figure 1B). In both HIV-negative and HIV-positive individuals, distributions of immune  
121 cells were significantly different between the two compartments (Figure 1C). In both groups,  
122 alveolar macrophages were the dominant immune cell in the bronchoalveolar compartment  
123 with medians of 87.4% (Interquartile range [IQR]: 79.8-90) and 79.3 (Interquartile range  
124 [IQR]: 70.9-88) among HIV-negative and HIV-positive persons, respectively (Figure 1C and  
125 Supplementary table 1). On the other hand, lymphocytes and neutrophils were the dominant  
126 immune cells in the peripheral blood in both groups. Notably, the distributions of major

127 immune cells were not significantly different between HIV-negative and HIV-positive  
128 participants within the compartments.

129 We then used flow cytometry to further assess if there were HIV-specific alterations within  
130 the lymphocyte populations. The proportions of total T cells (CD3<sup>+</sup> cells) were reduced in the  
131 peripheral blood mononuclear cells (PBMCs) but increased in bronchoalveolar lavage fluid  
132 cells (BLCs) of HIV-positive patients, consistent with HIV-associated T-cell infiltration in  
133 bronchoalveolar compartment (p = 0.0030 and p=0.0473, respectively) (Figure 1D). The  
134 reduction of proportions of CD3<sup>+</sup> lymphocytes in PBMCs of HIV-positive study participants  
135 was primarily due to the loss of CD4<sup>+</sup> T cells as shown by the reduction in proportions of  
136 CD4<sup>+</sup> T cells in PBMCs (p =0.0001). We observed similar reduction in proportions of CD4<sup>+</sup>  
137 T cells in the BLCs of HIV-positive participants (p <0.0001) (Figure 1E). Notably, we  
138 observed an HIV-associated increase in proportions of CD8<sup>+</sup> T cells in both PBMCs (p =  
139 0.002) and BLCs (p = <0.0001). In further separate analyses of the research bronchoscopy  
140 cohort and the hospital-based cohort, we observed a similar HIV-associated increase in  
141 proportions of CD8<sup>+</sup> T cells and a reduction in proportions of CD4<sup>+</sup> T cells in the BLCs and  
142 PBMCs (Supplementary figure 4 A, B, D and E). Thus, HIV was associated with an increase  
143 in proportions of CD8<sup>+</sup> T cells and a decrease in proportions of CD4<sup>+</sup> T cells in both blood  
144 and bronchoalveolar compartments in multiple cohorts.

145

146 HIV infection is associated with compartment-specific changes in the transcriptional profile  
147 in BLCs and PBMCs

148 To first assess transcriptome-wide differences between compartments, we used RNA-seq to  
149 determine RNA expression differences between BLCs and PBMCs in four HIV-uninfected  
150 participants and three HIV-infected participants from the hospital-based cohort. Except for

151 one PBMCs sample, we obtained at least 1 million unique forward and reverse reads for each  
152 sample after deduplication (Supplementary figure 2).

153 There were 4,761 differentially expressed genes (DEGs) between the BLCs and PBMCs in  
154 either HIV-positive or HIV-negative participants. Of these, there were 4,084 DEGs between  
155 BLCs and PBMCs in the HIV-negative group, with 2,336 genes being upregulated and 1,748  
156 genes being downregulated in BLCs when compared with PBMCs (Figure 2A). On the other  
157 hand, there were 2,186 DEGs between BLCs and PBMCs in the HIV-positive group, with  
158 1,204 genes being upregulated and 982 genes being downregulated in BLCs when compared  
159 with PBMCs (Figure 2B). Notably, the large majority of the DEGs (69% (1,509 out of  
160 2,186)) between compartments in the HIV-positive individuals were also differentially  
161 expressed between compartments in the HIV-negative individuals (Figure 2C).

162 To assess the compartment-specific effects of HIV, we then checked for differences between  
163 the HIV-negative and HIV-positive groups within each compartment. There were 774 DEGs  
164 in PBMCs between the HIV-positive and the HIV-negative groups, with 515 genes being  
165 upregulated and 259 genes being downregulated in the HIV-positive group (Figure 2D). On  
166 the other hand, there were 727 DEGs in BLCs in comparisons between the HIV-positive  
167 group and the HIV-negative group, with 540 genes being upregulated and 187 genes being  
168 downregulated in the HIV-positive group (Figure 2E). Notably, of the DEGs in either the  
169 BLCs or the PBMCs between disease states, only a very small minority (6.9%, 97 of 1401)  
170 were differentially expressed in both compartments. Thus, HIV-induced transcriptional  
171 alterations were compartment-specific (Figure 2F).

172 Using gene ontology (GO) analyses to annotate enriched functions in these compartment  
173 specific HIV-induced transcriptional changes, we identified 30 GO terms that were  
174 significantly enriched (FDR  $q$ -value $<0.05$ ) in our list of DEGs in PBMCs between the HIV-

175 positive and HIV-negative groups (Supplementary table 2). We also identified 140  
176 significantly enriched GO terms in BLCs between the HIV-positive and HIV-negative groups  
177 (Supplementary table 3). The top enriched GO term in the PBMCs of HIV-positive  
178 participants was the “type I interferon signaling pathway” gene set (Figure 3A). On the other  
179 hand, the most enriched GO term in the BLCs of HIV-positive participants was the “adaptive  
180 immune response” gene set (Figure 3B). We also observed some enrichment of the “response  
181 to interferon-beta” and “type I interferon signaling pathway” GO terms in the BLCs of HIV-  
182 positive participants, but those GO terms ranked low in our list (Supplementary table 3).  
183 Thus, even though HIV also induces a type I interferon signaling signature in  
184 bronchoalveolar compartment, its dominant effect there is the modulation of adaptive  
185 immune responses.

186 Enrichment of the “type I interferon signaling pathway” gene set in HIV-positive PBMCs  
187 was due to upregulation of twenty genes, namely *EGR1*, *IFI27*, *IFI35*, *IFI6*, *IFIT1*, *IFIT2*,  
188 *IFIT3*, *IFITM3*, *IRF4*, *IRF7*, *ISG15*, *MX1*, *MX2*, *OAS1*, *OAS2*, *OAS3*, *OASL*, *STAT1*, *XAF1*  
189 and *RSAD2*. On the other hand, enrichments of the “type I interferon signaling pathway” and  
190 the “response to interferon-beta” gene sets in HIV-positive BLCs were due to upregulation of  
191 fourteen genes, namely *EGR1*, *IFITM1*, *IFITM2*, *IFITM3*, *IRF1*, *IRF3*, *IRF4*, *IRF7*, *ISG15*,  
192 *ISG20*, *RSAD2*, *AIM2*, *CDC34* and *PYHIN1* (Figure 3C). Notably, from the above lists of  
193 twenty-eight type I interferon-associated genes that were differentially expressed in either of  
194 the two compartments, only six (namely *EGR1*, *IFITM3*, *IRF4*, *IRF7*, *ISG15*, and *RSAD2*)  
195 were differentially expressed in both compartments, suggesting qualitative differences  
196 between the compartments.

197 In BLCs, enrichment of the “adaptive immune response” gene set was attributable to the  
198 HIV-induced upregulation of transcripts that suggested infiltration with cytolytic T cells,  
199 such as the lineage transcripts for CD8<sup>+</sup> T cells (*CD3D*, *CD3E*, *CD3G*, *CD8A* and *CD8B*),

200 CD8<sup>+</sup> T-cell effector molecules (granzyme M (*GZMM*), perforin (*PRF1*) and interferon  
201 gamma (*IFNG*)) and the CD8<sup>+</sup> T-cell transcription factors (e.g. *EOMES*) (Figure 3C). We  
202 also observed contribution by inhibitory/exhaustion markers (PD-1 (*PDCDI*) and LAG-3  
203 (*LAG3*)) in the enrichment of this GO term. Further observation of B-cell transcripts (*CD19*,  
204 *CD79A* and *CD79B*) suggests that HIV also induces infiltration of the bronchoalveolar  
205 compartment by other lymphocytes as previously reported<sup>15</sup> (Figure 3C).

206 Since the GO analyses suggested lymphocyte infiltration into the bronchoalveolar  
207 compartment, we conducted further targeted analyses on the major lymphocyte lineage  
208 markers to determine the infiltrating populations. There were significant upregulations of  
209 *CD3D*, *CD3E*, *CD3G* and *CD19* transcripts in the BLCs but not PBMCs of HIV-positive  
210 patients, suggesting selective HIV-induced expansion in the bronchoalveolar compartment  
211 (Supplementary 3A-D). We observed significant upregulations of transcripts for *CD8A* and  
212 *CD8B* in both BLCs and PBMCs of HIV-positive patients (Supplementary 3E-F). Even  
213 though transcripts for *NCAMI/CD56* were reduced in PBMCs of HIV-positive patients, they  
214 were not significantly altered in BLCs, suggesting that the upregulation of cytotoxic markers  
215 in the BLCs of HIV-positive patients could be attributed to infiltration by cytotoxic CD8<sup>+</sup> T  
216 cells and not natural killer cells (Supplementary 3G). The levels of *CD4* transcripts did not  
217 differ between disease states in either of the compartments, probably because the molecule is  
218 expressed on CD4<sup>+</sup> T cells as well as other lineages such as monocytes and macrophages, a  
219 phenomenon that could mask the known HIV-induced CD4<sup>+</sup> T-cell depletion (Supplementary  
220 3H), with the latter confirmed by flow cytometry in PBMCs (Figure 1E).

221 The whole compartment transcriptomic approach limited our ability to confidently attribute  
222 the transcripts of effector molecules to any specific cell type, and in particular the infiltrating  
223 CD8<sup>+</sup> T cell population which appeared the most likely candidate based on transcriptome

224 profile. We therefore assessed the expression of these molecules in CD8<sup>+</sup> T cells using flow  
225 cytometry and RNA-seq on sorted CD8<sup>+</sup> T cells. At the protein level, HIV-positive people  
226 had higher levels of constitutive Granzyme B production in both PBMCs-derived and BLCs-  
227 derived CD8<sup>+</sup> T cells (Figure 4A). However, *ex vivo* stimulation with mitogens yielded  
228 similar inducible interferon gamma between the disease states in both PBMCs-derived and  
229 BLCs-derived CD8<sup>+</sup> T cells (Figure 4B). In agreement with our analyses on bulk BLCs, the  
230 HIV-positive individuals had increased expression of PD-1 in BLCs-derived CD8<sup>+</sup> T cells  
231 when compared with HIV-negative individuals (Figure 4C). Similar trends on PD-1  
232 expression were seen when we analyzed the two cohorts separately, confirming that they  
233 were immunologically similar (Supplementary figure 4 C and F). Transcriptional analysis of  
234 mRNA levels from sorted CD8<sup>+</sup> T cells confirmed these findings. HIV was associated with a  
235 trend of increased transcription for granzyme B (*GZMB*) in BLC-derived CD8<sup>+</sup> T cells  
236 (Figure 4D). Unlike the observation on inducible interferon gamma protein, we observed  
237 trends of higher constitutive expression of *IFNG* in HIV-positive individuals in both PBMCs-  
238 derived and BLCs-derived CD8<sup>+</sup> T cells, suggesting that HIV infection could be associated  
239 with increased constitutive transcription of *IFNG in vivo* (Figure 4E). In agreement with the  
240 data on expression of PD-1 protein on CD8<sup>+</sup> T cells, we observed a trend of HIV-associated  
241 increase in transcription of the PD-1 (*PDCDI*) in both BLCs-derived and PBMCs-derived  
242 CD8<sup>+</sup> T cells (Figure 4F). Thus, the infiltrating CD8<sup>+</sup> T cells in HIV-positive individuals'  
243 bronchoalveolar compartment had a functional phenotype consistent with pre-existing  
244 cytotoxic products. Considering that PD-1 can be a marker of both exhaustion and activation  
245 depending on context, the significance of increased PD-1 expression in BLC-derived CD8 T  
246 cells in the HIV-positive group needs to be determined in future studies.

247

248 **Discussion**

249 HIV is associated with an increased incidence of both infectious and non-infectious lung  
250 morbidities <sup>13, 16, 17</sup>. HIV-positive patients have a higher prevalence of *Pneumocystis*  
251 pneumonia, active tuberculosis, bacterial pneumonia and viral pneumonia <sup>13, 16</sup>. They also  
252 have a higher prevalence of noninfectious structural lung complications such as emphysema  
253 and chronic obstructive pulmonary disease (COPD) <sup>13, 17</sup>.

254 Despite the high prevalence of HIV-induced lung complications, the immunopathogenesis of  
255 HIV in the lung is poorly understood. Due to logistical difficulties of obtaining lung samples,  
256 most studies on immune responses to respiratory infections have been conducted in  
257 peripheral blood with an assumption that circulating cells have similarities with those in the  
258 lung. Here, we show that there are significant differences in the global transcriptional profiles  
259 between the blood and the bronchoalveolar compartment, and that the immunological effects  
260 of HIV infection revealed by whole compartment transcriptomics in the two compartments  
261 are different.

262 While a type I interferon signature was the most dominant effect of HIV in PBMCs, a CD8<sup>+</sup>  
263 T-cell infiltrate was the dominant effect in the bronchoalveolar compartment. We also  
264 observed a weaker and qualitatively different HIV-associated type I interferon signature in  
265 the bronchoalveolar compartment of viremic HIV patients. An elevated interferon signature  
266 in blood has been associated with progression to TB disease and could arguably relate to the  
267 increased susceptibility to TB disease among HIV patients who have a strong type I  
268 interferon signature in blood <sup>10</sup>. The qualitative differences in type I interferon signatures  
269 between the compartments could be due to the differences in cellular compositions. Whether  
270 specific lung signatures drive the association of type I interferon signaling with progression  
271 from latent to active TB remains largely unknown and can be addressed through the study of  
272 the bronchoalveolar compartment in participants who go on to develop TB disease.

273 The infiltration of the bronchoalveolar compartment of HIV-positive patients with CD8<sup>+</sup> T  
274 cells has been reported in previous studies. However, there is limited information on its  
275 functional nature <sup>15, 18</sup>. Using both flow cytometry and whole compartment and CD8<sup>+</sup> T cell  
276 specific RNA-seq, we show that the HIV-induced CD8<sup>+</sup> T-cell infiltrate is associated with  
277 higher expression of effector molecules such as granzymes, perforin and interferon gamma,  
278 suggesting a cytolytic and inflammatory profile. We also report higher expression of PD-1 on  
279 bronchoalveolar CD8<sup>+</sup> T cells of HIV-positive patients. PD-1 expression in CD8<sup>+</sup> T cells has  
280 been associated with exhaustion <sup>19</sup>. However, in juvenile idiopathic arthritis, PD-1<sup>+</sup> CD8<sup>+</sup> T  
281 cells derived from synovial fluid were metabolically active functional effector memory T  
282 cells, suggesting that PD-1 expression could also act as a marker of locally adapted functional  
283 T cells <sup>20</sup>. Thus, depending on context, PD-1 could be a marker of either exhaustion or local  
284 activation in tissues. Even though PD-1 blockade on BLCs-derived T cells from HIV-positive  
285 patients was previously shown to boost cytokine secretion *in vitro*, suggesting exhaustion,  
286 there was a counterintuitive increased PD-1 expression among the interferon gamma  
287 secreting T cells <sup>18</sup>. As such, the implication of HIV-associated increase in PD-1 expression  
288 on CD8<sup>+</sup> T cells in the bronchoalveolar compartment needs further investigation.

289 The HIV-induced infiltration of the bronchoalveolar compartment with cytolytic CD8<sup>+</sup> T  
290 cells could be driven directly by HIV replication <sup>21</sup>. The lung has been shown to be a site of  
291 HIV replication where small alveolar macrophages and CCR5 expressing CD4<sup>+</sup> T cells are  
292 preferentially infected with HIV <sup>9, 22</sup>. Infiltrating CD8<sup>+</sup> T cells could control local HIV  
293 replication by killing the HIV-infected CD4<sup>+</sup> T cells and alveolar macrophages. Indeed, in  
294 previous studies, lymphocytic alveolitis in asymptomatic HIV patients was enriched for HIV-  
295 specific cytotoxic CD8<sup>+</sup> T cells that could execute such effector functions <sup>18</sup>. Whether HIV  
296 induces bronchoalveolar infiltration with other specificities of CD8<sup>+</sup> T cells that can  
297 modulate opportunistic respiratory infections, such as tuberculosis, is unclear.

298 In other settings, CD8 lymphocytic alveolitis has been implicated in the pathogenesis of  
299 noninfectious lung complications, such as COPD and emphysema. Considering that HIV  
300 infection is also associated with increased prevalence of the same noninfectious lung  
301 complications, HIV-induced lymphocytic alveolitis is thought to accelerate the deterioration  
302 of lung function in patients who are exposed to other risk factors for COPD and emphysema,  
303 such as smokers<sup>21,23-26</sup>. Whether similar bystander destructive mechanisms play an important  
304 role in CD8<sup>+</sup> T-cell-mediated disruption of the containment of *Mycobacterium tuberculosis* in  
305 granulomas is unknown. In an immune-competent mouse model, LCMV-specific CD8<sup>+</sup> T  
306 cells infiltrated *Mycobacterium bovis* granulomas in the liver, but without conferring any  
307 benefit in the control of bacterial growth, suggesting that HIV-specific CD8<sup>+</sup> T cells in our  
308 setting could also infiltrate *Mycobacterium tuberculosis* granulomas in human hosts<sup>27</sup>. In  
309 another mouse model, LCMC-specific cytolytic CD8<sup>+</sup> T cells expressing granzyme B and  
310 NKG2D infiltrated *Leishmania major* lesions and exacerbated disease by causing an  
311 exaggerated inflammatory response<sup>28</sup>. Infiltrating cytolytic CD8<sup>+</sup> T cells in the lung of HIV  
312 patients could similarly exaggerate the inflammatory state, disrupting the containment of  
313 *Mycobacterium tuberculosis* in granulomas thus promoting bacterial dissemination. Notably,  
314 the CD8<sup>+</sup> T-cell infiltrate in our cohorts was characterized by increased expression of  
315 granzymes and perforin, suggesting some overlap between the findings in our cohorts and the  
316 *Leishmania major* mouse model<sup>28</sup>. Additional studies will be needed to directly interrogate  
317 the possible contribution of infiltrating CD8<sup>+</sup> T cells in the inflammatory destruction of lung  
318 tissues and the anatomical dissemination of *Mycobacterium tuberculosis* infections.

319 We conclude that HIV is associated with a cytolytic CD8<sup>+</sup> T-cell infiltrate in the  
320 bronchoalveolar compartment. Further mechanistic studies are required to understand the  
321 consequences of the infiltration on respiratory infections, such as *Mycobacterium*  
322 *tuberculosis*, and noninfectious comorbidities, such as COPD and emphysema. Our study did

323 not assess the antigen specificity of the infiltrating CD8<sup>+</sup> T cells, although a previous report  
324 suggested an enrichment for HIV-specific CD8<sup>+</sup> T cells<sup>18</sup>. In future studies, it will be  
325 important to determine whether enrichment for CD8<sup>+</sup> T cells against respiratory infections,  
326 such as *Mycobacterium tuberculosis* occurs, and the functional competence of these cell. This  
327 study was limited by the sample size in the transcriptomic profiling and intracellular cytokine  
328 staining. Nevertheless, the data reveal important compartment-specific effects of HIV in the  
329 bronchoalveolar compartment, suggesting a possible mechanism by which HIV modulates  
330 immunity to respiratory infections and lung function in ways that cannot be revealed by  
331 studying peripheral blood. Furthermore, we show the utility of using whole compartment  
332 transcriptomic analyses to reveal infiltration of different sites with various immune cells.

### 333 **Methods**

#### 334 Study population

335 We studied the effect of HIV on immune function in the peripheral blood and  
336 bronchoalveolar compartment using two bronchoalveolar study cohorts at African Health  
337 Research Institute (AHRI) in KwaZulu-Natal, South Africa. The first cohort was a hospital-  
338 based cohort in which we recruited HIV-negative or HIV-positive ART-naive participants  
339 (>18yrs) who came for clinical investigations but were determined (after extensive work-up  
340 including bronchoscopy and bronchoalveolar microbiological investigations) to not have any  
341 infectious or inflammatory pulmonary disease. Their clinical indications and final diagnosis  
342 are documented in supplemental table 4. Participants were consented for research use of  
343 clinically excess BAL fluid and a paired peripheral blood draw. The second cohort was a  
344 research bronchoscopy cohort of HIV-negative and HIV-positive adults (18-50yrs).  
345 Exclusion criteria included: pregnancy, any history of disease other than HIV, history of  
346 antiretroviral therapy (ART), and smoking. Study participants were recruited from  
347 KwaDabeka Community Health Centre. All participants were confirmed to be free of

348 respiratory symptoms and to have a normal chest x-ray. Further, HIV-positive participants  
349 were confirmed to have a negative sputum Mtb GeneXpert. The HIV status of all  
350 participants was determined by 4th generation HIV antibody/antigen Enzyme Linked-  
351 Immunosorbent Assay (ELISA) testing and HIV RNA quantitative viral load. CD4<sup>+</sup> T cell  
352 counts were determined in all participants. All participants also underwent assessment of  
353 hemoglobin (had at least 10g/dL), platelet level (had at least 100X10<sup>9</sup> cell/L) and  
354 prothrombin time (INR<1.3) to meet safety criteria for bronchoscopy. Once screened and  
355 characterized, participants were transported to Inkosi Albert Luthuli Central Hospital  
356 (IALCH) where they underwent research bronchoscopy and paired peripheral blood draw.  
357 All participants provided written informed consent. Both study protocols were approved by  
358 the University of KwaZulu-Natal Biomedical Research Ethics Committee (BREC; reference  
359 numbers BF503/15 and BE037/12) and Partners Institutional Review Board.

360

361 Participant samples were selectively subjected (depending on sample availability for different  
362 techniques) to differential cell count, mitogen stimulation, monoclonal antibody staining, and  
363 transcriptomic analysis.

364

#### 365 Sample processing and differential cell counts

366 Bronchoscopies were performed by pulmonologists at IALCH with participants receiving  
367 sedation and bronchodilators according to local standard of care protocols. Two hundred  
368 milliliters of normal saline were infused into the right middle lobe. Bronchoalveolar lavage  
369 fluid was stored at 4 °C and processed in the laboratory within 90 minutes. Paired peripheral  
370 blood was collected in acid citrate dextrose (ACD) tubes (BD, Franklin Lakes, NJ, USA) and  
371 stored at room temperature. A portion of the sample was directly used for differential cell  
372 counts in each compartment after standard preparation and interpretation of peripheral blood

373 smear and cytospin slide for BAL fluid. PBMCs were isolated using standard Histopaque  
374 (Sigma-Aldrich, St. Louis, MO, USA) gradient centrifugation protocols.

375 To isolate bronchoalveolar lavage fluid cells (BLCs), BAL fluid was passed through a 40 µm  
376 filter (BD). The fluid was spun at 1,500 RPM for 10 minutes at 4 °C and all cells resuspended  
377 in RPMI media supplemented with 5% fetal bovine serum, 1% penicillin/streptavidin, 1%  
378 HEPES buffer and 1% amphotericin. The cells were freshly used for monoclonal antibody  
379 staining and mitogen stimulation to test functionality.

380

### 381 Flow cytometry

382 The BLCs and PBMCs were counted and assessed for viability using trypan blue (Sigma-  
383 Aldrich) and compound microscopy to ensure > 90% lymphocyte viability. To assess  
384 distribution of CD4<sup>+</sup> and CD8<sup>+</sup> T cells, immune regulation and functionality of CD8<sup>+</sup> T cells  
385 in HIV infection, cells from the two compartments were subjected to two panels of  
386 fluorescently labelled antibodies. Panel 1 (phenotypic panel): Live/dead-amcyan (Life  
387 technologies, Carlsbad, CA, USA), CD3-BV650, CD4-BV711, CD14-APC-Cy7, PD-1-  
388 BV711, TIM-3-BV785 (Biolegend, San Diego, CA, USA) and CD8-PE Texas Red  
389 (Invitrogen, Carlsbad, CA, USA). Panel 2 (intracellular cytokine staining panel): Live/dead-  
390 amcyan (Life technologies), CD3-Alexa700, CD4-BV711, CD8-APC-Cy7, granzyme b-  
391 Alexa647, IFN $\gamma$ -Dazzle 549 (Biolegend). Panel 2 staining was done after stimulation with  
392 PMA/Ionomycin (25/500ng/mL). Acquisition was performed on BD FACS Aria III. Flowjo  
393 v10.5 (Flowjo, LLC) was used for flow cytometry analysis.

394

### 395 RNA isolation from Whole BAL

396 Freshly processed cellular pellets from bronchoalveolar lavage (1 mL of BAL fluid) and  
397 Histopaque gradient-isolated PBMCs (1 X 10<sup>6</sup> cells) from the hospital cohort for bulk

398 sequencing were stored in RNeasy lysis reagent (Qiagen) at -80 °C. Samples  
399 were later thawed at room temperature, pelleted and suspended with 1% β-mercaptoethanol  
400 RLT buffer from the RNeasy Micro kit (Qiagen, Hilden, Germany). Extraction of  
401 RNA was performed according to manufacturer's protocol. Briefly, a RNeasy spin column  
402 was used to homogenize the samples. DNase 1 treatment was used to eliminate any  
403 remaining genomic DNA contamination. The extracted RNA was quantified using nanodrop  
404 and aliquoted into ~200 ng aliquots, adequate for RNASeq library preparation. All aliquots  
405 were immediately stored at -80 °C.

406

#### 407 Sorted CD8<sup>+</sup> T cell populations

408 For work on purified CD8<sup>+</sup> T cells, freshly processed cells from the hospital cohort were  
409 sorted into 70% TRIzol LS Reagent (Thermo Fisher Scientific, Waltham, MA, USA) and  
410 stored at -80 °C. Both RNA and DNA were isolated from these samples using the  
411 TRIzol/chloroform method with minor modifications. Briefly, RNA was precipitated using a  
412 nucleic acid co-precipitant, 5 mg/mL linear acrylamide (Thermo Fisher Scientific). All  
413 reagents were kept at 4 °C to facilitate separation of nucleic acid into different layers and  
414 efficient precipitation. QIAGEN RNeasy Micro kit was used to purify RNA from the TRIzol  
415 extracted samples. The quality of the extracted RNA was determined using the BioAnalyzer  
416 RNA Pico kit (Agilent, Santa Clara, CA, USA).

417

#### 418 RNA-seq library preparation and sequencing

419 Enrichment for messenger RNA was done using the NEBNext Poly(A) mRNA Magnetic  
420 Isolation kit (New England Biolabs, Ipswich, MA, USA). RNA libraries were prepared using  
421 the NEBNext Ultra RNA Library Prep Kit for Illumina (New England Biolabs). Dual index

422 primers from the NEBNext Multiplex Oligos for Illumina kit were used to label the samples.  
423 A subset of the libraries was assessed for acceptable quality using the BioAnalyzer DNA  
424 High Sensitivity Chip or the DNA TapeStation (Agilent). Concentrations of the libraries were  
425 determined using a Qubit dsDNA assay kit (Thermo Fisher). Equal molarities of the indexed  
426 libraries were pooled and sequenced on an Illumina NextSeq 500 platform to yield 75 bp  
427 paired end reads.

428

#### 429 Sequencing data analyses

430 The raw data were demultiplexed and processed using Trimmomatic version 0.36 to remove  
431 adaptors and leading/trailing low-quality bases. Subsequent analyses were done using the  
432 Tuxedo protocol as previously described <sup>29</sup>. Briefly, the sequences were aligned on the  
433 human reference genome *GRCh37* (hg19) using the TopHat module (version 2.1.1) and  
434 bowtie (version 2.2.4). The mapped reads were then sorted using the Picard SortSam module.  
435 Duplicate reads were identified using the Picard MarkDuplicates module and removed. The  
436 Cufflinks module (Version 2.2.1) was used for subsequent analyses. The transcripts for each  
437 sample were assembled and the numbers of reads quantified for each transcript. The  
438 expression levels were expressed as Fragments Per Kilobase of transcript per Million  
439 fragments mapped (FPKM). The assembled transcripts for all samples were merged to obtain  
440 a master transcriptome assembly (Cuffmerge) followed by assessment of differential  
441 expression (Cuffdiff). A statistically significant difference in the expression of a transcript  
442 between two groups of participants was defined as having at least a two-fold difference and  $q$   
443  $< 0.05$  (after Benjamini-Hochberg correction for multiple-testing). CummeRbund R package  
444 (version 2.16), GraphPad Prism (version 8) and Morpheus-Broad Institute  
445 (<https://software.broadinstitute.org/morpheus/>) were used for subsequent data visualization.

446 Identification of HIV-induced pathway changes was done on the GOrilla platform ([http://cbl-](http://cbl-gorilla.cs.technion.ac.il/)  
447 [gorilla.cs.technion.ac.il/](http://cbl-gorilla.cs.technion.ac.il/)) by checking for enriched Gene Ontology (GO) terms among the  
448 differentially expressed genes<sup>30</sup>. To exclude very large or very small nonspecific GO terms  
449 that did not have specific biological implications, an arbitrary cut-off was set whereby only  
450 GO terms whose sizes are between 20 and 200 genes were considered in the analyses.

451

#### 452 Statistical analyses

453 Comparisons of flow cytometry data and differential counts data between HIV-uninfected  
454 and HIV-infected groups were assessed using the Wilcoxon rank-sum test. Matched  
455 comparisons of flow cytometry data and differential counts data between blood and  
456 bronchoalveolar lavage samples were assessed using the Wilcoxon matched pairs signed rank  
457 test. Differences were considered statistically significant if  $p < 0.05$ . Comparisons of ratios of  
458 participants between groups were done using Chi-square test. All statistical analyses were  
459 done on GraphPad Prism version 8 (GraphPad Software, Inc).

460

#### 461 **Acknowledgements**

462 This work was supported in part by grants from the South African Medical Research Council,  
463 the Department of Science and Technology/National Research Foundation Research Chairs  
464 Initiative, the Victor Daitz Foundation, a Burroughs-Wellcome Fund / American Society of  
465 Tropical Medicine and Hygiene fellowship, the National Institutes of Health (K08  
466 AI118538), the Harvard University Center for AIDS Research (grant P30 AI060354), a  
467 capacity building Strategic Award awarded to the KEMRI-Wellcome Trust Research  
468 Programme and the South Africa National Research Foundation. Additional support was

469 received through the Saharan African Network for TB/HIV Research Excellence (SANTHE),  
470 a DELTAS Africa Initiative [grant # DEL-15-006]. The DELTAS Africa Initiative is an  
471 independent funding scheme of the African Academy of Sciences (AAS)'s Alliance for  
472 Accelerating Excellence in Science in Africa (AESAs) and supported by the New Partnership  
473 for Africa's Development Planning and Coordinating Agency (NEPAD Agency) with  
474 funding from the Wellcome Trust [grant # 107752/Z/15/Z] and the UK government. The  
475 views expressed in this publication are those of the author(s) and not necessarily those of  
476 AAS, NEPAD Agency, Wellcome Trust or the UK government.

477

478 **Authors contributions**

479 D.M.M., Maphe Mthembu, A.S., U.S., S.S.R., B.C. and T.B. performed the experiments.  
480 K.N., D.F.K., P.M., Mohammed Mitha, M.S., Z.M., D.R., F.K. and Tarryn Naidoo collected  
481 the clinical samples. D.K., Thumbi Ndung'u and E.B.W. provided supervision. D.M.M.,  
482 Maphe Mthembu, Thumbi Ndung'u and E.B.W. wrote the manuscript. All authors reviewed  
483 the manuscript and approved the final version.

484 **Supplementary material**

485 All supplementary material and gene expression data are available at Figshare:

486 <https://figshare.com/s/e05711feb0360fe3ce33>

487

488 **Disclosure:** The authors declare no competing interests.

489

490 **References**

- 491 1. UNAIDS. DATA 2019; **Accessed 4th September 2019:**  
492 [https://www.unaids.org/sites/default/files/media\\_asset/2019-UNAIDS-data\\_en.pdf](https://www.unaids.org/sites/default/files/media_asset/2019-UNAIDS-data_en.pdf).  
493
- 494 2. UNAIDS. Tuberculosis and HIV. 2019; **Accessed 6th May 2019:**  
495 [https://www.unaids.org/sites/default/files/media\\_asset/tuberculosis-and-hiv-](https://www.unaids.org/sites/default/files/media_asset/tuberculosis-and-hiv-progress-towards-the-2020-target_en.pdf)  
496 [progress-towards-the-2020-target\\_en.pdf](https://www.unaids.org/sites/default/files/media_asset/tuberculosis-and-hiv-progress-towards-the-2020-target_en.pdf)  
497
- 498 3. Fenner L, Atkinson A, Boulle A, Fox MP, Prozesky H, Zurcher K *et al.* HIV viral load as  
499 an independent risk factor for tuberculosis in South Africa: collaborative analysis of  
500 cohort studies. *J Int AIDS Soc* 2017; **20**(1): 21327.  
501
- 502 4. Caruso AM, Serbina N, Klein E, Triebold K, Bloom BR, Flynn JL. Mice deficient in CD4 T  
503 cells have only transiently diminished levels of IFN-gamma, yet succumb to  
504 tuberculosis. *J Immunol* 1999; **162**(9): 5407-5416.  
505
- 506 5. Flynn JL, Chan J, Triebold KJ, Dalton DK, Stewart TA, Bloom BR. An essential role for  
507 interferon gamma in resistance to Mycobacterium tuberculosis infection. *The Journal*  
508 *of experimental medicine* 1993; **178**(6): 2249-2254.  
509
- 510 6. Sonnenberg P, Glynn JR, Fielding K, Murray J, Godfrey-Faussett P, Shearer S. How  
511 soon after infection with HIV does the risk of tuberculosis start to increase? A  
512 retrospective cohort study in South African gold miners. *The Journal of infectious*  
513 *diseases* 2005; **191**(2): 150-158.  
514
- 515 7. Day CL, Abrahams DA, Harris LD, van Rooyen M, Stone L, de Kock M *et al.* HIV-1  
516 Infection Is Associated with Depletion and Functional Impairment of Mycobacterium  
517 tuberculosis-Specific CD4 T Cells in Individuals with Latent Tuberculosis Infection. *J*  
518 *Immunol* 2017; **199**(6): 2069-2080.  
519
- 520 8. Jambo KC, Banda DH, Afran L, Kankwatira AM, Malamba RD, Allain TJ *et al.*  
521 Asymptomatic HIV-infected individuals on antiretroviral therapy exhibit impaired  
522 lung CD4(+) T-cell responses to mycobacteria. *American journal of respiratory and*  
523 *critical care medicine* 2014; **190**(8): 938-947.  
524
- 525 9. Jambo KC, Banda DH, Kankwatira AM, Sukumar N, Allain TJ, Heyderman RS *et al.*  
526 Small alveolar macrophages are infected preferentially by HIV and exhibit impaired  
527 phagocytic function. *Mucosal immunology* 2014; **7**(5): 1116-1126.  
528
- 529 10. Berry MP, Graham CM, McNab FW, Xu Z, Bloch SA, Oni T *et al.* An interferon-  
530 inducible neutrophil-driven blood transcriptional signature in human tuberculosis.  
531 *Nature* 2010; **466**(7309): 973-977.  
532
- 533 11. Sweeney TE, Braviak L, Tato CM, Khatri P. Genome-wide expression for diagnosis of  
534 pulmonary tuberculosis: a multicohort analysis. *The Lancet Respiratory medicine*  
535 2016; **4**(3): 213-224.  
536

- 537 12. Warsinske H, Vashisht R, Khatri P. Host-response-based gene signatures for  
538 tuberculosis diagnosis: A systematic comparison of 16 signatures. *PLoS medicine*  
539 2019; **16**(4): e1002786.  
540
- 541 13. Beck JM, Rosen MJ, Peavy HH. Pulmonary complications of HIV infection. Report of  
542 the Fourth NHLBI Workshop. *American journal of respiratory and critical care*  
543 *medicine* 2001; **164**(11): 2120-2126.  
544
- 545 14. Bosinger SE, Utay NS. Type I interferon: understanding its role in HIV pathogenesis  
546 and therapy. *Current HIV/AIDS reports* 2015; **12**(1): 41-53.  
547
- 548 15. Mwale A, Hummel A, Mvaya L, Kamng'ona R, Chimbayo E, Phiri J *et al.* B cell, CD8 (+)  
549 T cell and gamma delta T cell infiltration alters alveolar immune cell homeostasis in  
550 HIV-infected Malawian adults. *Wellcome open research* 2017; **2**: 105.  
551
- 552 16. Diedrich CR, Flynn JL. HIV-1/mycobacterium tuberculosis coinfection immunology:  
553 how does HIV-1 exacerbate tuberculosis? *Infection and immunity* 2011; **79**(4): 1407-  
554 1417.  
555
- 556 17. Staitieh B, Guidot DM. Noninfectious pulmonary complications of human  
557 immunodeficiency virus infection. *The American journal of the medical sciences*  
558 2014; **348**(6): 502-511.  
559
- 560 18. Neff CP, Chain JL, MaWhinney S, Martin AK, Linderman DJ, Flores SC *et al.*  
561 Lymphocytic alveolitis is associated with the accumulation of functionally impaired  
562 HIV-specific T cells in the lung of antiretroviral therapy-naive subjects. *American*  
563 *journal of respiratory and critical care medicine* 2015; **191**(4): 464-473.  
564
- 565 19. McLane LM, Abdel-Hakeem MS, Wherry EJ. CD8 T Cell Exhaustion During Chronic  
566 Viral Infection and Cancer. *Annual review of immunology* 2019; **37**: 457-495.  
567
- 568 20. Petrelli A, Mijnheer G, Hoytema van Konijnenburg DP, van der Wal MM, Giovannone  
569 B, Mocholi E *et al.* PD-1+CD8+ T cells are clonally expanding effectors in human  
570 chronic inflammation. *The Journal of clinical investigation* 2018; **128**(10): 4669-4681.  
571
- 572 21. Twigg HL, Soliman DM, Day RB, Knox KS, Anderson RJ, Wilkes DS *et al.* Lymphocytic  
573 alveolitis, bronchoalveolar lavage viral load, and outcome in human  
574 immunodeficiency virus infection. *American journal of respiratory and critical care*  
575 *medicine* 1999; **159**(5 Pt 1): 1439-1444.  
576
- 577 22. Corleis B, Bucsan AN, Deruaz M, Vrbanac VD, Lisanti-Park AC, Gates SJ *et al.* HIV-1  
578 and SIV Infection Are Associated with Early Loss of Lung Interstitial CD4+ T Cells and  
579 Dissemination of Pulmonary Tuberculosis. *Cell reports* 2019; **26**(6): 1409-1418  
580 e1405.  
581
- 582 23. Popescu I, Drummond MB, Gama L, Lambert A, Hoji A, Coon T *et al.* HIV Suppression  
583 Restores the Lung Mucosal CD4+ T-Cell Viral Immune Response and Resolves CD8+ T-

- 584 Cell Alveolitis in Patients at Risk for HIV-Associated Chronic Obstructive Pulmonary  
585 Disease. *The Journal of infectious diseases* 2016; **214**(10): 1520-1530.  
586
- 587 24. Petrache I, Diab K, Knox KS, Twigg HL, 3rd, Stephens RS, Flores S *et al.* HIV associated  
588 pulmonary emphysema: a review of the literature and inquiry into its mechanism.  
589 *Thorax* 2008; **63**(5): 463-469.  
590
- 591 25. Crothers K, Huang L, Goulet JL, Goetz MB, Brown ST, Rodriguez-Barradas MC *et al.*  
592 HIV infection and risk for incident pulmonary diseases in the combination  
593 antiretroviral therapy era. *American journal of respiratory and critical care medicine*  
594 2011; **183**(3): 388-395.  
595
- 596 26. Plata F, Autran B, Martins LP, Wain-Hobson S, Raphael M, Mayaud C *et al.* AIDS virus-  
597 specific cytotoxic T lymphocytes in lung disorders. *Nature* 1987; **328**(6128): 348-351.  
598
- 599 27. Hogan LH, Co DO, Karman J, Heninger E, Suresh M, Sandor M. Virally activated CD8 T  
600 cells home to Mycobacterium bovis BCG-induced granulomas but enhance  
601 antimycobacterial protection only in immunodeficient mice. *Infection and immunity*  
602 2007; **75**(3): 1154-1166.  
603
- 604 28. Crosby EJ, Goldschmidt MH, Wherry EJ, Scott P. Engagement of NKG2D on bystander  
605 memory CD8 T cells promotes increased immunopathology following *Leishmania*  
606 major infection. *PLoS Pathog* 2014; **10**(2): e1003970.  
607
- 608 29. Trapnell C, Roberts A, Goff L, Pertea G, Kim D, Kelley DR *et al.* Differential gene and  
609 transcript expression analysis of RNA-seq experiments with TopHat and Cufflinks.  
610 *Nature protocols* 2012; **7**(3): 562-578.  
611
- 612 30. Eden E, Navon R, Steinfeld I, Lipson D, Yakhini Z. GOrilla: a tool for discovery and  
613 visualization of enriched GO terms in ranked gene lists. *BMC bioinformatics* 2009; **10**:  
614 48.  
615

616

617

618

619

620

621

622

623 **Table 1: Demographic and clinical characteristics of the study population**

Characteristics	HIV-Negative	HIV-Positive	P-value
N	19	11	NA
Sex, # Females (%)	9 (47)	6 (54)	>0.9999
Age in years, median (IQR)	36 (32-44)	31 (30-40)	0.3883
CD4 counts in cells/ $\mu$ L, median (IQR)	1,048 (854-1,352)	353 (173-576)	<0.0001
Viral load in copies/mL, median (IQR)	0	54,942 (18,743-174,293)	NA

624 Data presented in median and interquartile range unless stated otherwise. Mann-Whitney U  
625 test was used to calculate significance between the two study groups. In the comparison for  
626 gender distribution between the groups, Chi-square test was used.

627 IQR: interquartile range

628 NA: not applicable

629

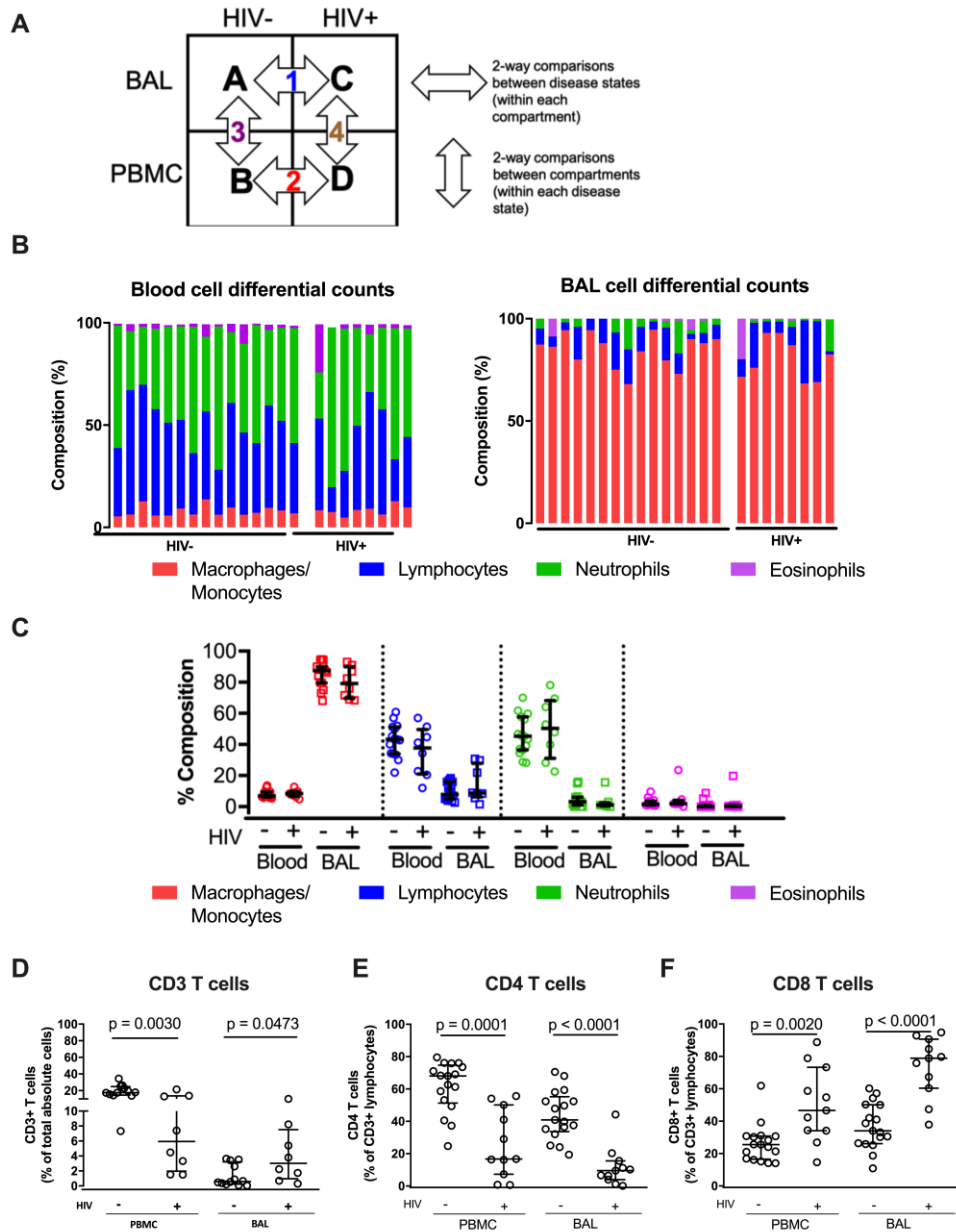


**Figure 1: Comparisons of the immune cell sub-types between peripheral blood and bronchoalveolar lavage (BAL) cells of both HIV-negative and HIV-positive individuals.** A) Two-way comparison of the study groups to understand inter-compartment differences and the impact of HIV on immune function. B) Proportion of immune cell subsets in the paired peripheral blood and bronchoalveolar cells in the HIV-negative (n=15) and HIV-positive groups (n=8). C) Quantitative comparison of panel B, showing level of significance between compartments in both HIV-negative and HIV-positive groups. D) Proportions of total absolute CD3+ T cells in BLCs and PBMCs in HIV-positive (n=8) and HIV-negative groups (n=15). E) Percentage CD4+ T cells of CD3+ T cells in BLCs and PBMCs in HIV-positive (n=11) and HIV-negative groups (n=19). F) Percentage of CD8+ T cells in BLCs and PBMCs in HIV-positive (n=11) and HIV-negative groups (n=19). The \* in the figures means p value was < 0.05.

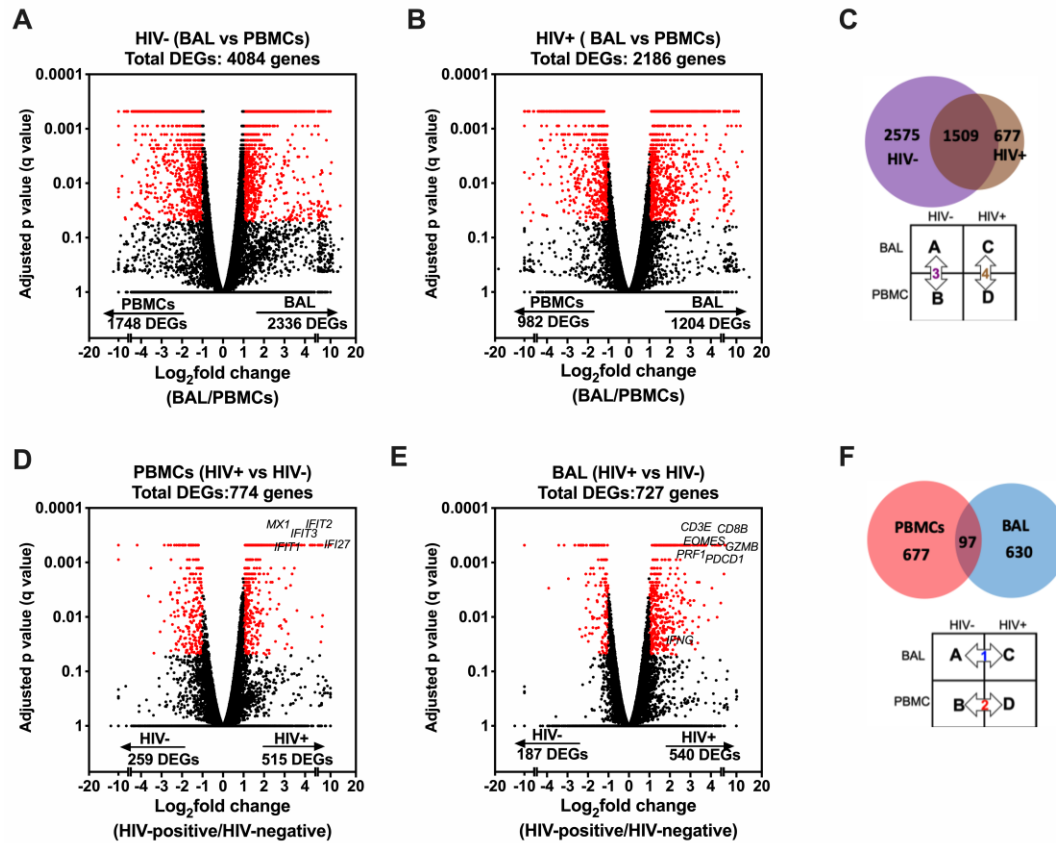
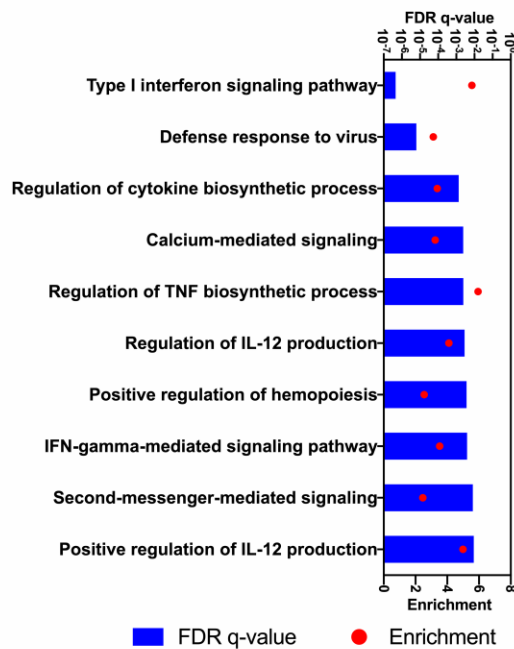
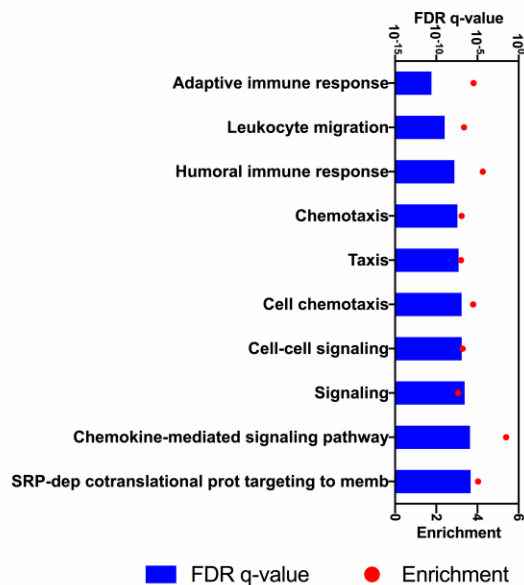


**Figure 2: Comparisons in transcriptomic profiles between bronchoalveolar lavage fluid cells (BLCs) and peripheral blood mononuclear cells (PBMCs) in HIV-infected and HIV-uninfected participants.** A) Differentially expressed genes between BLCs and PBMCs in the HIV-negative group (n=4). B) Differentially expressed genes between BLCs and PBMCs in the HIV-positive group (n=3). C) Numbers of differentially expressed genes between BLCs and PBMCs in both HIV-positive (n=3) and HIV-negative groups (n=4). D) Differentially expressed genes between HIV-negative (n=4) and HIV-positive (n=3) groups in PBMCs. E) Differentially expressed genes between HIV-negative and HIV-positive groups in BLCs. F) Numbers of differentially expressed genes between HIV-negative and HIV-positive groups in both PBMCs and BLCs.

### A PBMCs



### B BAL



### C

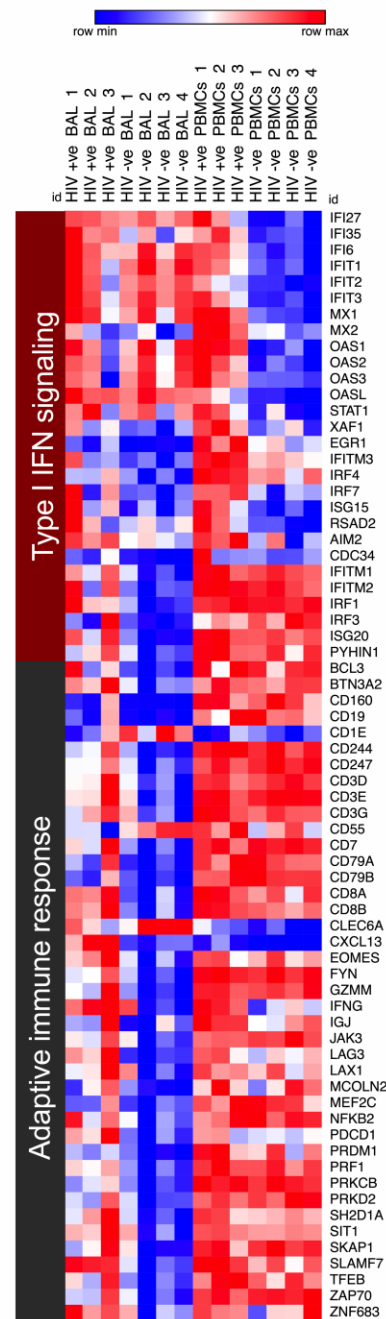


**Figure 3: Gene ontology analyses to identify HIV-induced enrichments in bronchoalveolar lavage fluid cells (BLCs) and peripheral blood mononuclear cells (PBMCs).** A) The top ten HIV-associated significantly enriched gene ontology (GO) terms in PBMCs. B) The top 10 HIV-associated significantly enriched gene ontology (GO) terms in BLCs. C) Heat map showing expression levels of the genes that contribute to the most enriched GO terms in PBMCs and BLCs i.e. “Type I interferon signaling pathway” and “Adaptive immune response”. Natural logarithms of (Expression level +1) were used.

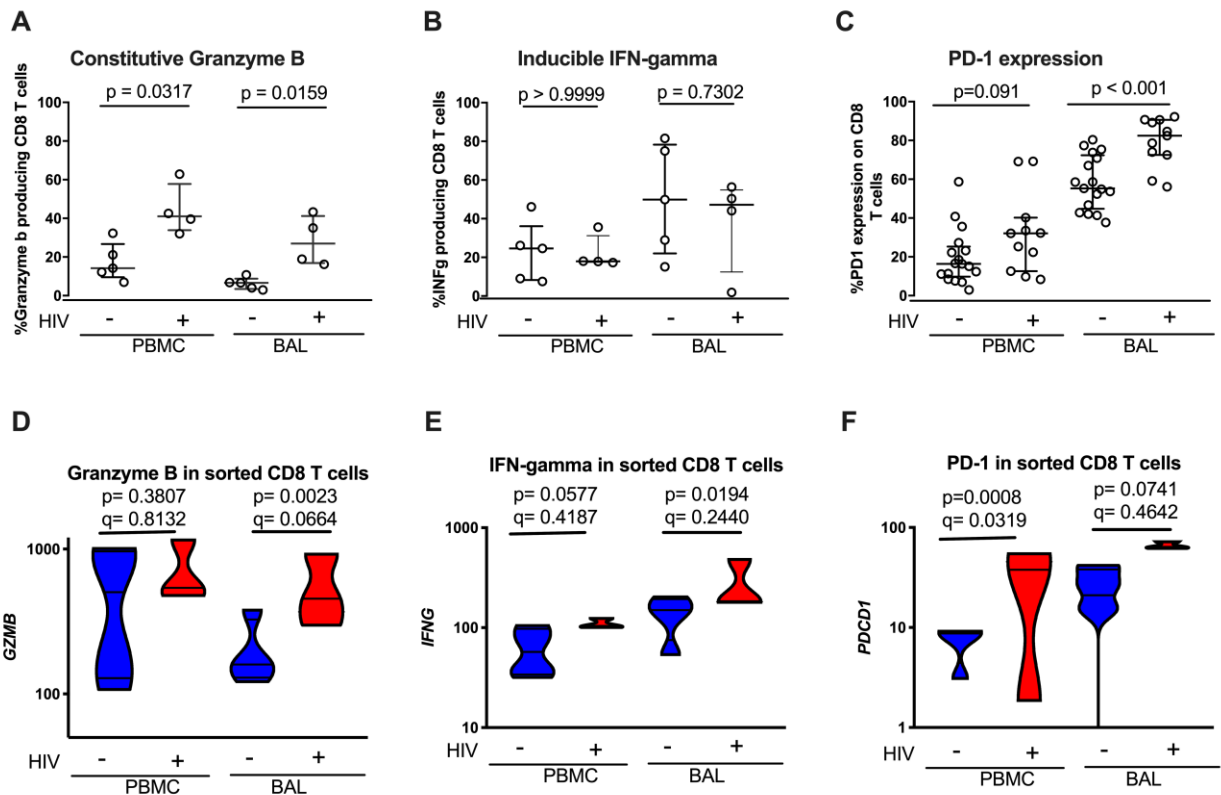


**Figure 4: Characterization of HIV-induced infiltrating CD8<sup>+</sup> T cells.** A) Constitutive expression of granzyme B in unstimulated CD8<sup>+</sup> T cells in PBMCs and BLCs from HIV-positive and HIV-negative participants. B) Expression of interferon gamma in unstimulated and stimulated CD8<sup>+</sup> T cells in PBMCs and BLCs from HIV-positive and HIV-negative participants. C) *Ex vivo* expression of PD-1 in CD8<sup>+</sup> T cells in PBMCs and BLCs from HIV-positive and HIV-negative participants. D) Expression levels of granzyme B mRNA (*GZMB*) in BLCs-derived sorted CD8<sup>+</sup> T cells and PBMCs-derived sorted CD8<sup>+</sup> T cells from HIV-positive and HIV-negative participants. E) Constitutive expression levels of interferon gamma mRNA (*IFNG*) in BLCs-derived sorted CD8<sup>+</sup> T cells and PBMCs-derived sorted CD8<sup>+</sup> T cells from HIV-positive and HIV-negative participants. F) Expression levels of PD-1 mRNA (*PDCD1*) in BLCs-derived and PBMCs-derived sorted CD8<sup>+</sup> T cells from HIV-positive and HIV-negative participants.